High-Strength Laminated Copper Matrix Nanocomposites Developed from a Single-Walled Carbon Nanotube Film with Continuous Reticulate Architecture

Zhiqiang Niu, Wenjun Ma, Jinzhu Li, Haibo Dong, Yan Ren, Duan Zhao, Weiya Zhou, and Sishen Xie**

A critical challenge in nanocomposite fabrication by adding SWCNTs as reinforcement is to realize an effective transfer of the excellent mechanical properties of the SWCNTs to the macroscale mechanical properties of the matrix. Using directly grown SWCNT films with continuous reticulate structure as the template, Cu/SWCNTs/Cu laminated nanocomposites are fabricated by an electrodepositing process. The resulting Cu/SWCNTs/Cu laminated nanocomposites exhibit extremely high strength and Young's modulus. The estimated Young's modulus of the SWCNT bundles in the composite are between 860 and 960 GPa. Such a high strength and an effective load-transfer capacity are ascribed to the unique continuous reticulate architecture of SWCNT films and the strong interfacial strength between the SWCNTs and Cu matrix. Raman spectroscopy is used to characterize the loading status of the SWCNTs in the strained composite. It provides a route to investigate the load transfer of SWCNTs in the metal matrix composites.

1. Introduction

Carbon nanotubes (CNTs) have high potential for improving the mechanical properties of composite materials due to its unique structure and remarkable mechanical properties with a tensile strength of 60 GPa and Young's modulus of 1 TPa.[1–4] A critical challenge in nanocomposite fabrication by adding SWCNTs as reinforcement is to realize effective transfer of the excellent mechanical properties of SWCNTs to the macroscale mechanical properties of the matrix.[5,6]

Progress has been made in SWCNT/polymer composites,[5,7–11] which exhibit a remarkable strengthening effect for the polymers due to the strong interfacial strength between the SWCNTs and the polymer matrix induced by their interaction at molecular level. However, it is difficult to fabricate SWCNT/metal composites with effective load transfer capacity due to the agglomeration of the SWCNTs in the matrix and the poor interfacial bonding because of a mere blending between SWCNTs and the metal matrix in the traditional powder-metallurgy processes.[12] It has been doubtful whether CNTs can really reinforce metals. Recently, several researchers have attempted novel routes to fabricate CNT-reinforced metal-matrix nanocomposites,[13–25] in particular, copper matrix nanocomposites, which can be applied to electrical contact materials because of their low thermal expansion, high electrical and thermal conductivity coefficient.[21,25] Although improvement has been achieved, the SWCNT reinforced metal nanocomposites have not shown the anticipated results because of the lack of a suitable synthesis technique to realize strong SWCNT/metal interface and homogenous dispersion of the SWCNTs in the metal matrix. It is suggested that the optimization of SWCNT/metal interface design and the orientation control of the SWCNTs in the matrix are the fundamental issues. Therefore, new approaches to a successful fabrication of SWCNT/metal nanocomposites should be explored to obtain a high degree of SWCNT dispersion in the metal matrix, a breakup of the SWCNT agglomerates, and a good wetting of SWCNTs with the matrix. Furthermore, an open issue associated with an in-depth understanding of the nanoscale mechanical interactions between SWCNTs and metal matrix and the loading status of the SWCNTs in the strained composites has to be faced.

In previous works, it has been proposed that if continuous macroscale SWCNT films or fibers were used to synthesize SWCNT-reinforced polymer composites, the load will be continuously and effectively transferred from the polymer matrix to the SWCNT films or fibers under moderate interface strength and the great strengthening effect for the composites would be achieved.[7,26,27] However, for the SWCNT-reinforced metal-matrix composites, it is rather difficult to control distribution and continuous structure of the SWCNTs in the composites by sintering or hot-pressing in traditional powder-metallurgy processes.[28,29] To control the distribution of SWCNTs in the composites, thin SWCNT film have been used to fabricate

Dr. Z. Q. Niu, Dr. W. J. Ma, J. Z. Li, H. B. Dong, Y. Ren, D. Zhao, Prof. W. Y. Zhou, Prof. S. S. Xie
Beijing National Laboratory for Condensed Matter Physics, Institute of Physics
Chinese Academy of Sciences
Beijing 100190, China
E-mail: wyzhou@iphy.ac.cn; ssxie@iphy.ac.cn
J. Z. Li, H. B. Dong, Y. Ren, D. Zhao
Graduate School of the Chinese Academy of Sciences
Beijing 100039, China

DOI: 10.1002/adfm.201201532

polymer or metal-matrix composites.[14,15,30] But the SWCNT films such as bucky paper used to fabricate composites is not continuous. Besides, surfactants were also attached on the surface of SWCNTs, which have severe impact on SWCNTs/matrix interface. As a result, SWCNT membrane reinforced composites have shown only moderate enhancement in modulus and strength. Recently, we improved the floating catalyst chemical vapor deposition (FCCVD) technique and fabricated the freestanding SWCNT films with high conductivity.[31] These directly grown SWCNT films possess unique continuous reticulate structure, which is different from the post-deposited SWCNT films. It has been demonstrated that this continuous reticulate structure displayed a better strengthening effect for the composites in comparison to randomly dispersed short CNTs.[7,32] If the metal matrix composite is fabricated based on this continuous reticulate architecture, excellent mechanical properties may be achieved. Therefore, it is of great significance to propose a strategy to apply the directly fabricated SWCNTs films to the metal-matrix composite and improve the load-transfer efficiency of the SWCNTs in the metal-matrix composite.

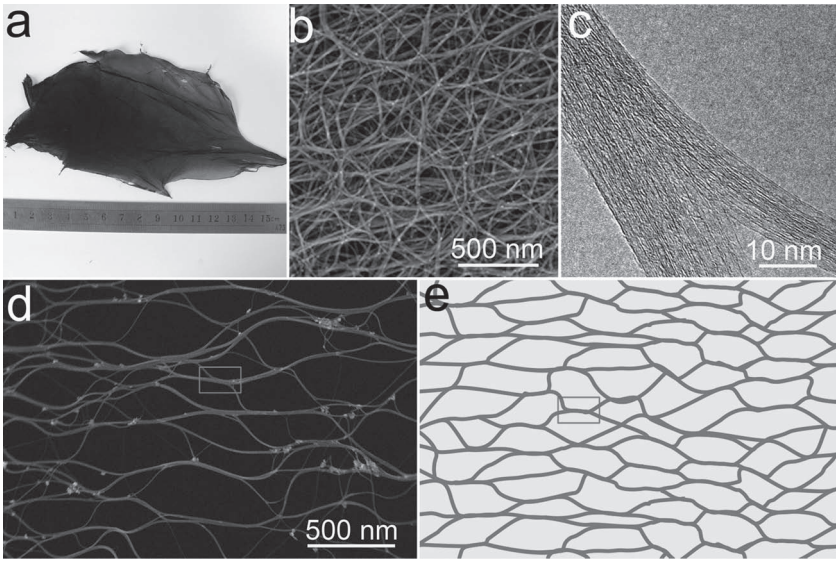

Figure 1. a) Optical, b) SEM and c) TEM images of the as-prepared SWCNT film. d) SEM images of SWCNT bundles peeled off from thick SWCNT film. e) Schematic illustration of the internal architecture of the processed SWCNT film reinforced composite.

In this paper, we report a simple and effective method to fabricate Cu/SWCNT/Cu sandwich-type laminated nanocomposites by electrodeposition using freestanding SWCNT films with continuous reticulate structure as template. By this method, the SWCNT films in Cu/SWCNT/Cu laminated nanocomposites can not only keep continuous reticulate structure within the plane easily, but the orientation control of SWCNTs can be realized also. The continuous reticulate architecture of the SWCNT films and the strong interfacial strength between the SWCNT and Cu matrix result in an effective load-transfer capacity of the SWCNT bundles in the laminated nanocomposites. The estimated Young's modulus of the SWCNT bundles in the composite are in the range of 860–960 GPa. Such a high load-transfer efficiency leads to the extremely high mechanical properties of the laminated composites. The loading status of the SWCNTs in metal-matrix composite during strain was successfully characterized by Raman spectroscopy, which provides a route to investigate the load transfer of SWCNTs in the metal matrix composite.

2. Results and Discussion

The SWCNT films used in this work were fabricated by FCCVD as described in our earlier work.[31] Large area and free-standing characteristics of the SWCNT films bring the convenience for its practical application (**Figure 1**a). The scanning electron microscopy (SEM) image of a SWCNT film (Figure 1b) shows a nanoporous architecture, which would be of great importance for the filling of Cu-matrix and the bridging between the upper and lower layers of the matrix. The transmission electron microscopy (TEM) image of the SWCNT film (Figure 1c) shows that the sidewall of SWCNTs is almost free from the impurities such as amorphous carbon. Clean sidewalls play an important role in the formation of high interfacial strength because the impurities on surface of SWCNTs block the direct interfacial contact between SWCNTs and metal matrix and severely affect the formation of strong interfacial bonding.[33] The unique continuous reticulate structure of the directly grown SWCNT films (Figure 1d), different from the short and random-oriented structure of post-deposited SWCNT film such as Bucky papers, will undoubtedly benefit the load-transfer efficiency in laminated nanocomposites.

However, similar to the result reported,[34] the surface of as-prepared SWCNTs is hydrophobic, so that aqueous solutions would not completely penetrate and access the interspaces of the film and wet the surface of SWCNTs easily, which blocks the Cu filling in the interspaces of the film and the formation of strong interfacial bonding between SWCNTs and the Cu matrix. In previous reports, surfactants were widely used to disperse CNTs and to enhance the hydrophilic property of CNTs by attaching to the surface of CNTs.[14] Although the positive metal ions can form chemical bonds with the negative wrapped SWCNTs by the surfactants, positive metal ions can not directly form strong interfacial bonding with SWCNTs due to the surfactants between them, which may have adverse effects on the load-transfer efficiency in the composites. To overcome these deficiencies, the directly fabricated SWCNT films were treated in air at 450 °C for 3 h before preparing Cu/SWCNTs/Cu laminated nanocomposites. Heat-treatment of SWCNTs could make the surface of SWCNTs more hydrophilic owing to the presence of functional group. So that the aqueous solution can penetrate and access the interspaces of the film easily and contact the surface of SWCNTs better.[35] Furthermore, the metal ions can form strong bonding with the functional groups on the surface of SWCNTs.[13]

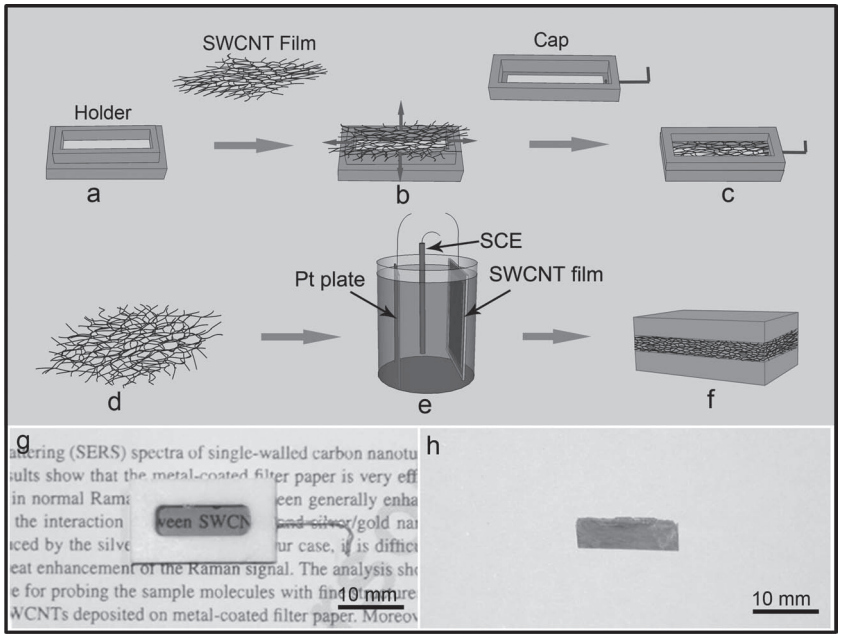

Figure 2. Schematic process of spreading out SWCNT film flatly (a–c) and electrodepositing Cu using SWCNT film as template (d–f). g) Optical images of the SWCNT film fixed between "holder" and "cap" and h) the Cu/SWCNT/Cu laminated nanocomposite.

Since the inhomogeneous dispersion of the SWCNT embedded in the metal matrix has a severe effect on the mechanical performance of the composites,[13,14] it is required that the film keeps flat in the preparing process of composite by electrodeposition. However, when the as-grown SWCNT film dips directly into the solution, they would gather into a mass due to the surface tension between SWCNT film and the solution. To successfully spread out SWCNT films, a strategy for processing directly grown SWCNT films is proposed. **Figure 2**a–c schematically depict the method by which the SWCNT film can be spread out flatly and easily. The SWCNT film was first spread out onto a hollow holder which has two layers with different length and width. Since the SWCNT film is free-standing onto the hollow of holder and can not attach onto any substrates, SWCNT film can be easily drawn on all sides in a plane and makes the SWCNT film flat, as depicted in Figure 2b. After drawing the film flatly, a "cap" was covered onto the holder to fix the film, as shown in Figure 2c. Figure 2g is the optical image of a SWCNT film in a holder. To illustrate the availability of this method, a thin SWCNT film with uniform transparence was shown in Figure 2g. If the films are not well flat, due to the severe diffusion, they will lose homogeneous transparence even if they are thin enough. Furthermore, this approach can also avoid the agglomeration of SWCNT film and the formation of wrinkles in the electrolyte. Therefore, the SWCNT layer in laminated nanocomposites is homogeneous in a plane. Figure 2d–f schematically show the electrodepositing process of Cu matrix. Electrodeposition of Cu was performed in a traditional three-electrode cell, in which a platinum plate, a saturated Calomel electrode (SCE) and a SWCNT film were used as the counter, reference and working electrodes, respectively, as shown in Figure 2e. In previous reports,[14] the SWCNT films were deposited onto other substrates as working electrode template. So Cu can only be electrodeposited on one side of film because only one side of film can contact the electrolyte and the electrolyte just diffuse into the film from one side. However, for electrodepositing process shown in Figure 2e, the electrolyte can contact both sides of film and diffuse into the film from both sides. Therefore, Cu can be effectively filled into the interspace of film and the Cu layers can be achieved on both sides of film.

The mechanical properties of pure SWCNT film and Cu/SWCNTs/Cu laminated nanocomposites were tested on a tensile testing machine (Instron 5848) and the results are shown in **Figure 3**a and b, respectively. The pure SWCNT film exhibits good toughness and higher tensile strength than typical bucky paper due to its unique continuous reticulate structure.[31,36] Figure 3b shows the mechanical properties of pure Cu film and Cu/SWCNTs/Cu laminated nanocomposites with different volume fraction of SWCNTs. Both the tensile strength and the Young's modulus of Cu/SWCNTs/Cu

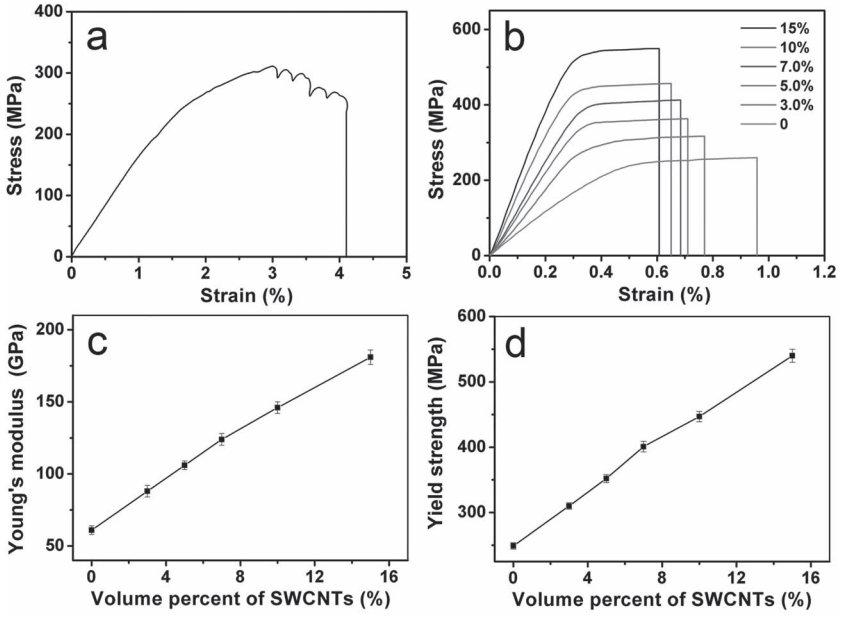

Figure 3. a) Mechanical properties of pure SWCNT film. b) Mechanical properties of pure Cu film and Cu/SWCNTs/Cu laminated nanocomposites. c) Young's modulus and d) yield strength of the Cu/SWCNTs/Cu laminated nanocomposites with different volume percentage of the SWCNTs.

Table 1. Experimental and estimated Young's modulus of Cu/SWCNTs/Cu composites and SWCNT bundles in the composite at different volume percent of SWCNTs

Young's modulus			Volume percent	
Cu/SWCNTs/Cu composite (GPa)[a]	Cu (GPa)[a]	SWCNTs (GPa)[b]	Cu (%)[a]	SWCNTs (%)[a]
181	61	860	85	15
146	61	911	90	10
124	61	961	93	7
106	61	960	95	5
88	61	936	97	3

[a]Experimental result; [b]Estimated result.

laminated nanocomposites are much higher than those of the Cu specimen, which was fabricated by the same method as Cu/SWCNTs/Cu laminated nanocomposites. In the case of 15 vol.%, both the tensile strength and the Young's modulus are about 3 times as high as those of the Cu specimen. They are also higher than those of Cu/SWCNTs/Cu laminated nanocomposites prepared by other method.[14] Moreover, both the tensile yield strength and the Young's modulus of Cu/SWCNTs/Cu laminated nanocomposites increased as the volume fraction of SWCNTs was increased, as shown in Figure 3c,d.

The Young's modulus (E) of the composites can be calculated by the following equation:[15]

$$E = E_f V_f + E_m V_m \quad (1)$$

where E_f and V_f are the Young's modulus and the volume fraction of the reinforcing phase (SWCNTs), respectively, and E_m and V_m are the Young's modulus and volume fraction of the Cu matrix. According to Equation 1, the E_f values at different volume fraction of SWCNT film are estimated as listed in **Table 1**. The estimated E_f values are in a range of 860–960 GPa. Such remarkable load-transfer efficiency results in the high tensile yield strength and the Young's modulus of Cu/SWCNTs/Cu laminated nanocomposites. The estimated E_f values of SWCNT in the Cu/SWCNTs/Cu laminated nanocomposites are larger than that of pure SWCNT film. It is ascribed to the filling of the Cu in the interspaces of the SWCNT film, which can effectively avoid the deformation process of the SWCNT film and make the macroscale strain come from the axial extension of SWCNTs rather than from the deformation of the SWCNT film.

The unique reticulate architecture of the SWCNT films (Figure 1d) used in this work plays an important role for such remarkable load-transfer efficiency. This unique reticulate architecture has its advantage on load transferring over a large area.[7] If the metal matrix composites can be prepared based on such SWCNT films with continuous reticulate architecture (schematically illustrated in Figure 1e), the load could be continuously transferred through the network rather than merely through SWCNT/Cu interfaces. In this case, the strength of the interbundle junctions in a SWCNT continuous network will play an important role in the load transferring. Figure 1d reveals that reticulate structure in the macroscale SWCNT films are assembled by SWCNT bundles through strong Y-type interbundle junctions (marked by red rectangle), by which the load could be continuously transferred through the network. Strong Y-type interbundle junctions ensure that local stress could be transferred across SWCNT networks through interbundle shear-lag so that the load will be continuously and effectively transferred from the matrix to the SWCNT film under moderate interface strength. Therefore, a great strengthening effect for the composites could be successfully achieved. In contrast, in the case of post-deposited SWCNT films, they have very weak junctions and the surface of SWCNTs was attached by surfactants. The random-oriented structure and the weak interbundle junctions result in the moderate enhancement in modulus and strength of the metal-matrix composites based on the post-deposited SWCNT films.[14] Undoubtedly, composites based on directly fabricated SWCNT films with continuous reticulate structure would exhibit a significant improvement in the mechanical properties in comparison with that based on post-deposited SWCNT films.

The strong interfacial strength between the SWCNTs and Cu matrix is another key factor for the high load-transfer capacity. Hydrophilic and clean SWCNT surface makes Cu ions directly contact the surface of SWCNTs easily and forms strong interface between the SWCNTs and Cu matrix during electrodeposition. Furthermore, functional groups were formed on the surface of SWCNTs because of the heat-treatment for the SWCNTs.[37] The metal ions can form strong bonding with the functional groups on the surface of SWCNTs,[13] which would also enhance the interfacial strength between the SWCNTs and Cu matrix. Strong interfacial strength is inferred by the SEM image of the fracture edge of the laminated nanocomposites (**Figure 4**a) and the energy dispersive X-ray (EDX) spectrum (Figure 4b) of the SWCNT pullout at the fracture. Figure 4a displays the typical damage mechanism under tensile loading. Figure 4b is the EDX spectrum at marked position by rectangle at the fracture edge in Figure 4a. In Figure 4b, Cu, C and Si are observed. Si is ascribed to the Si substrate on which the laminated nanocomposites with fracture edge was fixed to test

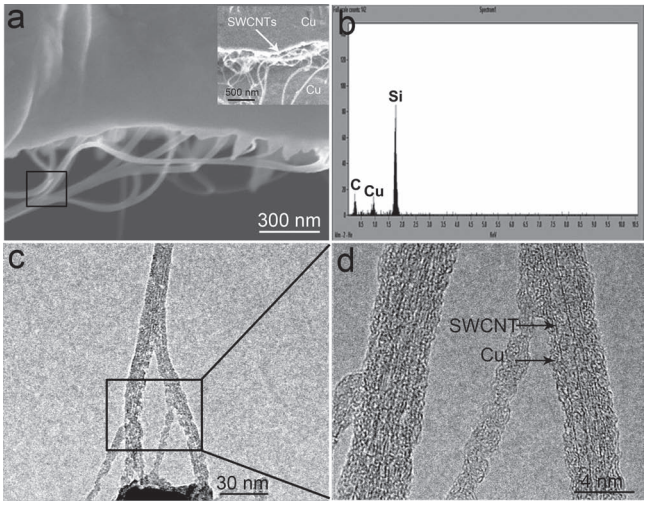

Figure 4. a) SEM and cross-section SEM (inset) images and b) EDX spectrum of the fracture edge of the laminated nanocomposites. TEM images of the SWCNT pullout at the fracture edge at c) low and d) high magnifications.

SEM and EDX spectrum. Both Cu and C are attributed to the SWCNT pullout at the fracture edge of the laminated nanocomposites. It indicates that Cu exists on the surface of the SWCNT pullout, which illustrates the strong interfacial strength between the SWCNTs and Cu matrix. The strong interfacial strength ensures that potential mechanical properties of SWCNTs can be transferred to the Cu matrix.

For an in-depth understanding of the SWCNT pullout at the fracture edge, the TEM of the SWCNT pullout was performed. Figure 4c,d are the TEM images of the SWCNT pullout at the fracture edge at low and high magnifications, respectively. Compared to the pure SWCNTs (Figure 1c), Figure 4c,d show that a layer of Cu was observed on the surface of the SWCNT pullout at the fracture edge. It also indicates that strong interfacial strength between the SWCNTs and Cu matrix were successfully achieved during the electrodeposition.

The mechanical performance of SWCNT-reinforced metal matrix composites essentially relies on the loading status of the SWCNTs in the composite. Therefore, it is crucial to understand the loading status of the SWCNTs in the composite during strain. Raman spectroscopy is a simple and powerful technique to identify and study SWCNT products.[38] Since Raman scattering (G′ band) is sensitive to the inter-atomic distance and there is a linear relationship between the shift of Raman peaks and the local strain,[39,40] it has been successfully applied to characterize the local strain of CNTs in the polymer matrix through the shift of Raman peaks.[7] However, the CNT-reinforced metal-matrix composite fabricated by conventional methods have low content of CNTs. Besides, when the bulky composite were strained, it is difficult to apply Raman to test CNTs in the strained composite. As a result, Raman characterization for loading status of the CNTs in the CNT-reinforced metal-matrix composites under the strain is rather hard to realize. Our thin Cu/SWCNTs/Cu laminated nanocomposite film successfully overcome above problems. Raman spectra (G′ band) of SWCNTs in the Cu/SWCNTs/Cu laminated nanocomposites were measured under different strains through a novel method (shown in the experimental section). **Figure 5** shows the G′ bands of SWCNTs in Cu/SWCNTs/Cu laminated nanocomposites under different strains. The downshifts of the G′ band were observed with the increase of the strains. Since the downshifts of the G′ band arise from the weakening of the carbon-carbon bonds as a result of the elongated inter-atomic distance, the macroscale strain contributed by the axial extension of SWCNTs can be inferred by the value of the downshift rate of the G′ band with respect to strain. Figure 5 shows that the downshift of the G′ band increases linearly at a rate of 27 cm^{-1} per 1% strain for the Cu/SWCNT/Cu laminated nanocomposites. It is about 5 times higher than that of SWCNT-reinforced polymer matrix composite,[7] which indicates that the load-transfer efficiency of SWCNTs in metal matrix is effectively enhanced in comparison with the case of polymer matrix composites. However, the downshift of the G′ band for the SWCNTs in Cu/SWCNT/Cu laminated nanocomposites is smaller than the average downshift rate of the G′ band for strained individual SWNT bundle, which is 37.3 cm^{-1} per 1% strain.[41] The reason may be that in the tensile-loading experiment for strained individual SWNT bundle, the SWCNT bundle's strain was completely in the loading direction. However, the orientation of the SWCNT bundles in the Cu/SWCNTs/Cu laminated nanocomposites is not completely along the direction of the macroscale strain, which is originated from the component of the axial extension of SWCNTs. Therefore, the misalignment of the SWCNT bundles in the Cu matrix is the main reason for the decrease of load-transfer efficiency in comparison with that of individual SWNT bundle. Besides, in Figure 5a, no obvious asymmetrical broadening of the line shape for the G′ band was observed for the strained composite, even under the max-strained case. It is different from the case of pure SWCNT film as reported in our earlier work.[39] It indicates that no deformation process of the SWCNT film occurred during the strain in the Cu/SWCNT/Cu laminated nanocomposites. The filling of the Cu in the interspace of the SWCNT film can effectively avoid the deformation process of the SWCNT film and make the macroscale strain come from the axial extension of SWCNTs rather than from the deformation of the SWCNT film. It is helpful for the improvement of the mechanical properties of Cu/SWCNTs/Cu laminated nanocomposites.

It is worth noting that this method is of extremely easy manipulability and could be applicable to other metal-matrix composites and a wide range of functional materials, such as conducting polymer.

3. Conclusions

Cu/SWCNTs/Cu laminated nanocomposites were fabricated by an electrodepositing process using directly fabricated SWCNT films as the template. The resulting Cu/SWCNTs/Cu laminated nanocomposites exhibit extremely high strength and Young's modulus. The estimated Young's modulus of the SWCNT bundles in the composite are in the range of 860–960 GPa, indicating that the laminated nanocomposites realize the effective transfer of the outstanding mechanical properties of SWCNTs to the Cu matrix. Continuous reticulate architecture of SWCNT films and the strong interfacial strength between the SWCNTs and Cu matrix are responsible for the extremely high strength and effective load-transfer capacity. The loading status of the SWCNTs in the

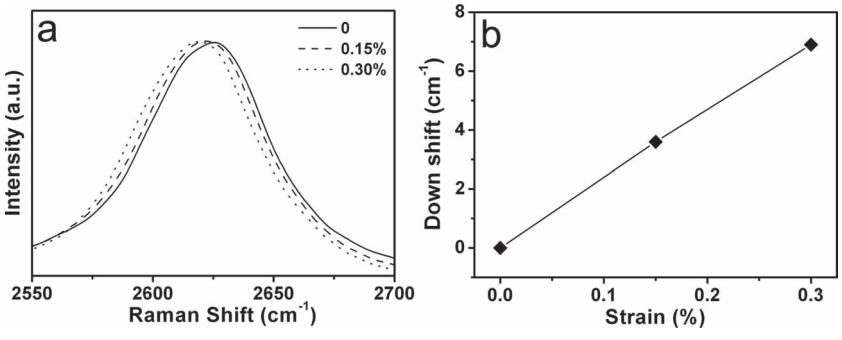

Figure 5. a) G′ bands of SWCNTs in Cu/SWCNT/Cu laminated nanocomposites under different strains. b) Downshift of G′ bands under different strains.

strained composite was successfully characterized by Raman spectroscopy. It provides a route to investigate the load transfer of SWCNTs in the metal matrix composites. This method is of extremely easy manipulability and could be applicable to other metal-matrix composites and a wide range of functional materials.

4. Experimental Section

Preparation of the SWCNT Film: The SWCNT films were prepared by FCCVD method, as reported previously.[31] In brief, ferrocene/sulfur powder as catalyst source, with a molar rate 16:1, was heated to 70–80 °C. The sublimed catalyst was carried by the mixture of flowing argon (1000 sccm) and methane (8 sccm) into the reaction zone. The growth rates of the films are mainly determined by the sublimation rate of the catalysts. The temperature of quartz tube was set at 1100 °C. After 3h, the reactor was cooled to room temperature in Ar atmosphere (50 sccm), and SWCNT films could be carefully peeled off from the wall of the quartz tube. Heat-treated SWCNTs films were obtained by heating as-prepared SWCNT films in air at 450 °C for 3 h.

Preparation of Cu/SWCNTs/Cu Laminated Nanocomposites: The SWCNT films with about 400 nm thickness were first fixed between the "holder" (size: 2.3 cm × 1.3 cm) and "cap" (size: 2.3 cm × 1.3 cm), as shown in Figure 2. The size of the hollow in "holder" and "cap" was 1.5 cm × 0.5 cm. Then electrodeposition of Cu was performed at galvanostatic mode with a constant current density of 15 mA cm^{-2} in a traditional three-electrode cell. A platinum plate, a saturated Calomel electrode (SCE) and SWCNT film were used as the counter, reference and working electrodes, respectively. Electroplating was performed in an electrolyte of $CuSO_4{\cdot}6H_2O$ (200 g L^{-1}) and sulfuric acid (H_2SO_4) (30 g L^{-1}), chloride ions (70 ppm) and brightener for acidic copper plating at room temperature. To deposit pure Cu film, a layer of Au film (100 nm) was first deposited on a glass substrate. Then electroplating Cu was performed using Au film as working electrode by the same method as depositing Cu on SWCNT films. Finally, Freestanding Cu film was obtained by peeling Cu film from glass substrate.

Characterization of Cu/SWCNT/Cu Laminated Nanocomposites: The tensile tests of the SWCNT films and Cu/SWCNT/Cu laminated nanocomposites were performed on an Instron 5848 microtester (5 N load cell). The gauge length and width were fixed at 1 cm and 1 mm, respectively, and the extension rate was 0.15% per min. The thickness of Cu/SWCNTs/Cu laminated nanocomposites was determined from SEM images before performing tensile tests. The volume fraction of the SWCNT film in the composites can be calculated by:

$$V_f = T_s\,(1 - x)\,/\,T \qquad (2)$$

where V_f is the volume fraction of the reinforcing SWCNT film, T_s is the thickness of reinforcing SWCNT film, x is the free volume of the pure SWCNT film, and T is the thickness of the laminated nanocomposites. As reported previously, the free volume (x) of the pure SWCNT film is about 25%.[31] The thickness of reinforcing SWCNT film (T_s) and the laminated nanocomposites (T) can be obtained from SEM images. So the volume fraction (V_f) of the reinforcing SWCNT film can be calculated by Equation 2. The morphology and the microstructure of the fracture edge of the laminated nanocomposites were examined by SEM (Hitachi S-5200) with energy-disperse X-ray spectrum analysis system (EDX, Thermoelectron USA) and TEM (JEOL JEM-2010). To measure the Raman spectra of SWCNTs in composites, the Cu/SWCNTs/Cu laminated composites have to be thinned from one side of the composites to the layer of SWCNTs by fine sandpaper due to the limitation of the detection depth of Raman. The Raman spectra of the strained nanocomposites were recorded with spectrophotometer (Renishaw inVia). The operating wavelength is 633 nm.

Acknowledgements

This work was supported by the National Basic Research Program of China (2012CB932302), the National Natural Science Foundation of China (51172271, 90921012), and Beijing Municipal Education Commission (YB20108000101).

Received: June 7, 2012
Published online: August 8, 2012

[1] P. M. Ajayan, *Chem. Rev.* **1999**, *99*, 1787.
[2] P. M. Ajayan, J. M. Tour, *Nature* **2007**, *447*, 1066.
[3] A. G. Souza, N. Kobayashi, J. Jiang, A. Gruneis, R. Saito, S. B. Cronin, J. Mendes, G. G. Samsonidze, G. G. Dresselhaus, M. S. Dresselhaus, *Phys. Rev. Lett.* **2005**, *95*, 217403.
[4] M. F. Yu, O. Lourie, M. J. Dyer, K. Moloni, T. F. Kelly, R. S. Ruoff, *Science* **2000**, *287*, 637.
[5] P. Podsiadlo, A. K. Kaushik, E. M. Arruda, A. M. Waas, B. S. Shim, J. D. Xu, H. Nandivada, B. G. Pumplin, J. Lahann, A. Ramamoorthy, N. A. Kotov, *Science* **2007**, *318*, 80.
[6] G. D. Zhan, J. D. Kuntz, J. L. Wan, A. K. Mukherjee, *Nat. Mater.* **2003**, *2*, 38.
[7] W. J. Ma, L. Q. Liu, Z. Zhang, R. Yang, G. Liu, T. H. Zhang, X. F. An, X. S. Yi, Y. Ren, Z. Q. Niu, J. Z. Li, H. B. Dong, W. Y. Zhou, P. M. Ajayan, S. S. Xie, *Nano Lett.* **2009**, *9*, 2855.
[8] A. A. Mamedov, N. A. Kotov, M. Prato, D. M. Guldi, J. P. Wicksted, A. Hirsch, *Nat. Mater.* **2002**, *1*, 190.
[9] M. T. Byrne, Y. K. Gun'ko, *Adv. Mater.* **2010**, *22*, 1672.
[10] Q. F. Cheng, M. Z. Li, L. Jiang, Z. Y. Tang, *Adv. Mater.* **2012**, *24*, 1838.
[11] A. B. Dalton, S. Collins, E. Munoz, J. M. Razal, V. H. Ebron, J. P. Ferraris, J. N. Coleman, B. G. Kim, R. H. Baughman, *Nature* **2003**, *423*, 703.
[12] E. Neubauer, M. Kitzmantel, M. Hulman, P. Angerer, *Compos. Sci. Technol.* **2010**, *70*, 2228.
[13] S. I. Cha, K. T. Kim, S. N. Arshad, C. B. Mo, S. H. Hong, *Adv. Mater.* **2005**, *17*, 1377.
[14] T. J. Kang, J. W. Yoon, D. I. Kim, S. S. Kum, Y. H. Huh, J. H. Hahn, S. H. Moon, H. Y. Lee, Y. H. Kim, *Adv. Mater.* **2007**, *19*, 427.
[15] Y. H. Li, W. Housten, Y. M. Zhao, Y. Q. Zhu, *Nanotechnology* **2007**, *18*, 205607.
[16] K. T. Kim, J. Eckert, S. B. Menzel, T. Gemming, S. H. Hong, *Appl. Phys. Lett.* **2008**, *92*, 121901.
[17] B. Lim, C. J. Kim, B. Kim, U. Shim, S. Oh, B. H. Sung, J. H. Choi, S. Baik, *Nanotechnology* **2006**, *17*, 5759.
[18] C. N. He, N. Q. Zhao, C. S. Shi, X. W. Du, J. J. Li, H. P. Li, Q. R. Cui, *Adv. Mater.* **2007**, *19*, 1128.
[19] G. Yamamoto, M. Omori, T. Hashida, H. Kimura, *Nanotechnology* **2008**, *19*, 315708.
[20] K. T. Kim, S. Il Cha, T. Gemming, J. Eckert, S. H. Hong, *Small* **2008**, *4*, 1936.
[21] Q. Ngo, B. A. Cruden, A. M. Cassell, G. Sims, M. Meyyappan, J. Li, C. Y. Yang, *Nano Lett.* **2004**, *4*, 2403.
[22] L. Jiang, Z. Q. Li, G. L. Fan, L. L. Cao, D. Zhang, *Carbon* **2012**, *50*, 1993.
[23] Z. Y. Liu, B. L. Xiao, W. G. Wang, Z. Y. Ma, *Carbon* **2012**, *50*, 1843.
[24] S. Arai, Y. Suwa, M. Endo, *J. Electrochem. Soc.* **2011**, *158*, D49.
[25] S. R. Bakshi, D. Lahiri, A. Agarwal, *Int. Mater. Rev.* **2010**, *55*, 41.
[26] L. Ci, J. Suhr, V. Pushparaj, X. Zhang, P. M. Ajayan, *Nano Lett.* **2008**, *8*, 2762.
[27] H. G. Chae, S. Kumar, *Science* **2008**, *319*, 908.
[28] T. W. Scharf, A. Neira, J. Y. Hwang, J. Tiley, R. Banerjee, *J. Appl. Phys.* **2009**, *106*, 013508.
[29] K. T. Kim, S. Il Cha, S. H. Hong, *Mater. Sci. Eng., A* **2006**, *430*, 27.
[30] J. H. Gou, *Polym. Int.* **2006**, *55*, 1283.

[31] W. J. Ma, L. Song, R. Yang, T. H. Zhang, Y. C. Zhao, L. F. Sun, Y. Ren, D. F. Liu, L. F. Liu, J. Shen, Z. X. Zhang, Y. J. Xiang, W. Y. Zhou, S. S. Xie, *Nano Lett.* **2007**, *7*, 2307.

[32] J. Z. Li, Y. Gao, W. J. Ma, L. Q. Liu, Z. Zhang, Z. Q. Niu, Y. Ren, X. X. Zhang, Q. S. Zeng, H. B. Dong, D. Zhao, L. Cai, W. Y. Zhou, S. S. Xie, *Nanoscale* **2011**, *3*, 3731.

[33] J. A. Kim, D. G. Seong, T. J. Kang, J. R. Youn, *Carbon* **2006**, *44*, 1898.

[34] D. N. Futaba, K. Hata, T. Yamada, T. Hiraoka, Y. Hayamizu, Y. Kakudate, O. Tanaike, H. Hatori, M. Yumura, S. Iijima, *Nat. Mater.* **2006**, *5*, 987.

[35] J. Li, A. Cassell, L. Delzeit, J. Han, M. Meyyappan, *J. Phys. Chem. B* **2002**, *106*, 9299.

[36] P. M. Ajayan, L. S. Schadler, C. Giannaris, A. Rubio, *Adv. Mater.* **2000**, *12*, 750.

[37] E. Lafuente, M. A. Callejas, R. Sainz, A. M. Benito, W. K. Maser, M. L. Sanjuan, D. Saurel, J. M. de Teresa, M. T. Martinez, *Carbon* **2008**, *46*, 1909.

[38] A. M. Rao, E. Richter, S. Bandow, B. Chase, P. C. Eklund, K. A. Williams, S. Fang, K. R. Subbaswamy, M. Menon, A. Thess, R. E. Smalley, G. Dresselhaus, M. S. Dresselhaus, *Science* **1997**, *275*, 187.

[39] W. J. Ma, L. Q. Liu, R. Yang, T. H. Zhang, Z. Zhang, L. Song, Y. Ren, J. Shen, Z. Q. Niu, W. Y. Zhou, S. S. Xie, *Adv. Mater.* **2009**, *21*, 603.

[40] S. B. Cronin, A. K. Swan, M. S. Unlu, B. B. Goldberg, M. S. Dresselhaus, M. Tinkham, *Phys. Rev. Lett.* **2004**, *93*, 167401.

[41] S. B. Cronin, A. K. Swan, M. S. Unlu, B. B. Goldberg, M. S. Dresselhaus, M. Tinkham, *Phys. Rev. B* **2005**, *72*, 035425.